Strain Birefringence in Real Elastomeric Networks: Modifications of Theory and Comparison to Experimental Data

Ronald O. Neaffer and Vassilios Galiatsatos*

Institute of Polymer Science, University of Akron, Akron, Ohio 44325-3909

Received January 19, 1993; Revised Manuscript Received April 20, 1993

ABSTRACT: A theory of strain birefringence in real elastomeric networks was previously proposed by one of us. The theory was based upon the modified constrained chain theory of rubberlike elasticity developed by Erman and Monnerie. Recent modifications have been made to the constrained chain theory which necessitate alterations in the affected portions of the theory of strain birefringence. Those alterations and their effect on predicted birefringence are examined. The modified predictions of the strain birefringence theory will be examined and compared to both experimental data and the original predictions of the theory. The agreement with experiment is found to be satisfactory.

Introduction

The phantom and affine models of amorphous networks represent only an approximation to real elastomeric networks.[1] An improvement over these models is the constrained junction theory of Flory[2,3] and Erman,[3] which incorporates the effect of topological constraints (entanglements) acting upon network junction fluctuations into the network elastic free energy. The constrained junction theory was extended by Erman and Monnerie into the constrained chain theory.[4] The constrained chain theory accounts for constrained fluctuations along the network chain contour instead of restricting the constraints to acting only upon the network junctions. The constrained chain theory was the basis for a theory of strain birefringence in real elastomeric networks proposed previously by one of us.[5]

The development and predictions of the previously proposed strain birefringence theory are reexamined in this paper due to recent modifications made to the constrained chain theory.[6] The constrained chain theory is reviewed in the first section, with the recent modifications being noted. The application of the constrained chain theory to the development of the strain birefringence theory is examined in the following two sections of the paper. Section two considers the phantom network contribution to birefringence, while section three considers the contribution to birefringence by the constraints. The resultant predictions of the theory of strain birefringence are presented and discussed in the next section. This section includes representative calculations that allow the application of the theory to experiment, as well as examination of the effect of constraints and swelling on the predictions of the theory. Finally, the theory is compared with experimental data.

Constrained Chain Theory

The constrained chain theory of rubberlike elasticity[4] is based upon Flory's hypothesis that only those entanglements (topological constraints) which are affected by deformation will contribute to the equilibrium network modulus.[2] The theory considers the network chains to be composed of Gaussian subchains. Topological constraints are allowed to act upon the end points of these subchains anywhere along the chain contour. The earlier constrained junction theory[7] restricted the topological constraints to acting only upon the multifunctional cross-linking junctions. The constrained chain theory incorporates the effect of topological constraints along the chain contour into the calculation of the network elastic free energy.

The elastic free energy due to the topological constraints is given by[4]

$$\Delta A_c = (\nu kT/2)\sum_t [B_t + D_t - \ln(1 + B_t) - \ln(1 + D_t)] \qquad \text{for } t = x, y, z \quad (1)$$

where ν is the number of network chains, k is the Boltzmann constant, and T is the absolute temperature. The functions B_t and D_t are defined as[4,8]

$$B_t = [h(\lambda_t)^2((K_G/h(\lambda_t))\lambda_t^2 - 1)]/[\lambda_t^2 + h(\lambda_t)]^2 \qquad \text{for } t = x, y, z \quad (2)$$

$$D_t = \lambda_t^2 B_t/h(\lambda_t) \qquad \text{for } t = x, y, z \quad (3)$$

where the variable λ_t represents the "t" component of the macroscopic deformation tensor. For uniaxial deformation λ_t is defined as[7]

$$\lambda_x = (V_{2c}/V_2)^{1/3}\alpha \quad (4)$$

$$\lambda_y = \lambda_z = (V_{2c}/V_2)^{1/3}\alpha^{-1/2} \quad (5)$$

where V_{2c} and V_2 are the polymer volume fractions present during cross-linking and experiment, respectively, and α is the extension ratio characterizing the amount of deformation. The function $h(\lambda_t)$ is defined as[6]

$$h(\lambda_t) = K_G[1 + (\lambda_t^2 - 1)\Phi] \qquad \text{for } t = x, y, z \quad (6)$$

where the variable K_G is the only adjustable parameter of the constrained chain theory of rubberlike elasticity if the cycle rank ξ is known (as in a model network). The parameter K_G is connected to network characteristics and is a measure of the strength of the constraints which affect the fluctuations of the network chains. The parameter K_G is defined as[4]

$$K_G = \langle(\Delta X_G)^2\rangle_0/\langle(\Delta x_G)^2\rangle_0 \quad (7)$$

where the numerator in eq 7 represents the mean of the squared unidirectional fluctuation of the center of mass of an undeformed chain from the average location in a phantom network. The denominator in eq 7 represents the mean of the squared unidirectional fluctuation of the center of mass of an undeformed chain from the average position subject to topological constraints. The function Φ from eq 6 can be defined in two ways

$$\Phi = [1 - (2/\phi)]^2/3 \quad (8)$$

0024-9297/93/2226-4013$04.00/0

$$\Phi = [1 - (2/\phi)]^2 \quad (9)$$

where ϕ is the functionality of the network cross-link junctions. The choice between eqs 8 and 9 is dependent upon the type of fluctuations considered to be occurring at the end points of the Gaussian subchains. Given sufficiently long chains, eq 8 is valid for subchain end-point fluctuations which are independent of macroscopic deformation[9-11] (referred to as the standard constrained chain model). Equation 9 is valid for subchain end-point fluctuations which are dependent upon macroscopic deformation (referred to as the modified constrained chain model). It should be noted that, in the latter case, the fluctuations of the cross-link junctions remain invariant with strain.[12,13]

Phantom Network Birefringence

The birefringence induced in a network under deformation consists of contributions from both the phantom network and the topological constraints. First consider the phantom network birefringence. In a perfect phantom network the birefringence due to deformation is[1]

$$\Delta n_{ph} = (2\pi/27)(\nu/V)[\Gamma_2(n^2+2)^2/n][\Lambda_{x,ph}^2 - (\Lambda_{y,ph}^2 + \Lambda_{z,ph}^2)/2] \quad (10)$$

In eq 10, ν represents the number of network chains, V corresponds to the network volume, and n is the network mean refractive index. The variable Γ_2 is the anisotropic parameter and is related to the polarizability tensor by[14]

$$[\alpha_{xx} - (\alpha_{yy} + \alpha_{zz})/2]_r = \Gamma_2[x^2 - (y^2 + z^2)/2]/\langle r^2\rangle_0 \quad (11)$$

where $\langle r^2\rangle_0$ is the mean-squared end-to-end distance of a free chain. The orthogonal components of the anisotropic portion of the polarizability tensor, when averaged over all conformations for a chain with fixed ends, are represented by α_{xx}, α_{yy}, and α_{zz} in eq 11. The Λ_t variables in eq 10 are the "t" directional components of the phantom network molecular deformation tensor defined as[1]

$$\Lambda_{t,ph}^2 = [1 - (2/\phi)]\lambda_t^2 + (2/\phi) \qquad \text{for } t = x, y, z \quad (12)$$

where λ_t and ϕ have been previously defined.

The stress-optical coefficient, C, is given by[7,15]

$$C = (2\pi/27kT)[\Gamma_2(n^2+2)^2/n] \quad (13)$$

By substituting eqs 12 and 13 into eq 10, the birefringence due to deformation in a phantom network is

$$\Delta n_{ph} = (\xi/V)kTC[\lambda_x^2 - (\lambda_y^2 + \lambda_z^2)/2] \quad (14)$$

where the cycle rank ξ is defined as

$$\xi = \nu[1 - (2/\phi)] \quad (15)$$

When limiting concern to the two principal axes, x and y, the birefringence due to the phantom network is given by

$$\Delta n_{xy,ph} = (\nu/V)kTC[1 - (2/\phi)](\lambda_x^2 - \lambda_y^2) \quad (16)$$

Birefringence Due to Constraints

The birefringence induced in a network under deformation consists of contributions from both the phantom network and the topological constraints.[7] Consider now the birefringence due to constraints. The topological constraints contribute to the molecular deformation tensor. The constraint portion of the molecular deformation tensor was previously defined as[7]

$$\Lambda_{t,c}^2 = (2/\phi)B_t \qquad \text{for } t = x, y, z \quad (17)$$

However, eq 17 has been found to underestimate the effect of the constraints.[6,8] Equation 17 assumes, by analogy to the corresponding equation in constrained junction theory, that the constraint contribution to the network elastic free energy is proportional to μ, the number of junctions

$$\mu = (2/\phi)\nu \quad (18)$$

when in the constrained chain theory it is actually proportional to ν, the number of chains. Therefore, the constraint portion of the molecular deformation tensor in the constrained chain model is correctly defined as[8]

$$\Lambda_{t,c}^2 = B_t \qquad \text{for } t = x, y, z \quad (19)$$

The contribution to the birefringence along the two principal axes by the constraint portion of the molecular deformation tensor is

$$\Delta n'_{xy,c} = (\nu/V)kTC(\Lambda_{x,c}^2 - \Lambda_{y,c}^2) \quad (20)$$

By substituting eq 19 into eq 20, the effect of constrained network deformation on birefringence is given by

$$\Delta n'_{xy,c} = (\nu/V)kTC(B_x - B_y) \quad (21)$$

There also exists a second type of contribution to birefringence as a result of topological constraints. Since the dimensions of the network chains are altered upon deformation, the end points of the Gaussian subchains should move correspondingly. Assuming the subchain end points and the constraint domains surrounding them behave as elastically coupled elements, the domains will react to movement of the subchain end points. This reaction should result in some additional orientation that contributes to birefringence. This additional orientation has been previously characterized by a domain deformation tensor θ, defined as[7]

$$\theta^2 = 1 + D_t \qquad \text{for } t = x, y, z \quad (22)$$

where D_t is given by eq 3. The contribution to birefringence along the two principal axes by this additional orientation has been previously defined as[4,5]

$$\Delta n''_{xy,c} = b(\nu/V)kTC(D_x - D_y) \quad (23)$$

where the parameter b is a scaling factor with no clear molecular connection. The value of b is in the range [0,1], and it is used due to the difficulty in determining the extent to which the domain deformation actually contributes to the birefringence due to constraints.[7]

Combining eq 21 and 23 gives the total birefringence due to constraints

$$\Delta n_{xy,c} = \Delta n'_{xy,c} + \Delta n''_{xy,c} \quad (24)$$

$$\Delta n_{xy,c} = (\nu/V)kTC(B_x - B_y) + b(\nu/V)kTC(D_x - D_y) \quad (25)$$

Substitution of eq 3 into eq 25 yields

$$\Delta n_{xy,c} = (\nu/V)kTC(B_x - B_y) + b(\nu/V)kTC\{\lambda_x^2 B_x[h(\lambda_x)]^{-1} - \lambda_y^2 B_y[h(\lambda_y)]^{-1}\} \quad (26)$$

$$\Delta n_{xy,c} = (\xi/V)kTC\{1/[1 - (2/\phi)]\}\{(B_x - B_y) + b(\lambda_x^2 B_x[h(\lambda_x)]^{-1} - \lambda_y^2 B_y[h(\lambda_y)]^{-1})\} \quad (27)$$

The total birefringence of a real network is the sum of the birefringence due to the phantom network and the birefringence due to constraints[7]

$$\Delta n_{xy} = \Delta n_{xy,ph} + \Delta n_{xy,c} \quad (28)$$

The total birefringence of a real network can also be defined

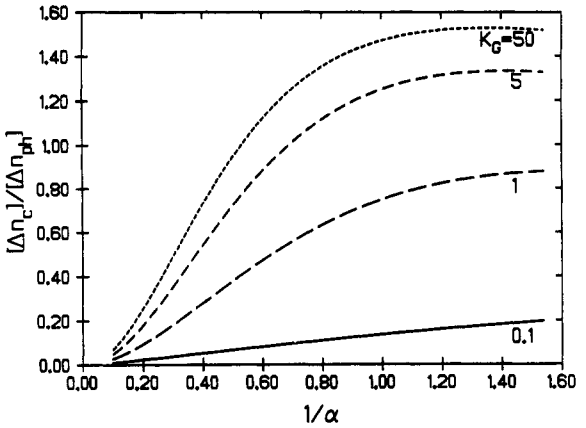

Figure 1. Effect of the primary constraint parameter, K_G, on representative results. See text for calculation details.

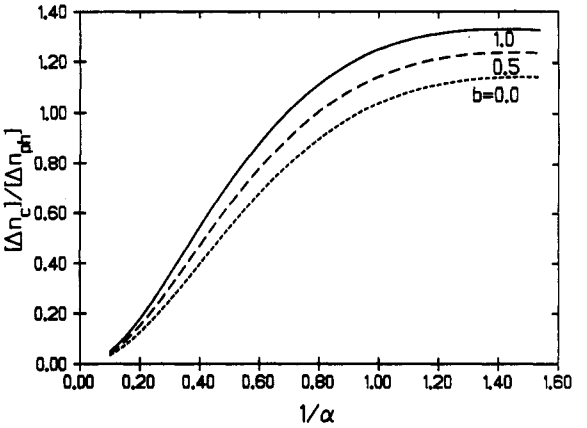

Figure 2. Effect of the secondary constraint scaling parameter, b, on representative results. See text for calculation details.

as[7]

$$\Delta n_{xy} = (\nu/V)kTC[(\Lambda_{x,\mathrm{eff}})^2 - (\Lambda_{y,\mathrm{eff}})^2] \quad (29)$$

where the terms inside the brackets in eq 29 are the two principal components of the total effective molecular deformation tensor defined below

$$\Lambda_{t,\mathrm{eff}}^2 = (\Lambda_{t,\mathrm{ph}})^2 + (\Lambda_{t,c})^2 + b(\theta_t^2 - 1) \qquad \text{for } t = x, y, z \quad (30)$$

which by substitution of eqs 12, 19, and 22 yields

$$(\Lambda_{t,\mathrm{eff}})^2 = [1 - (2/\phi)]\lambda_t^2 + (2/\phi) + B_t + b\lambda_t^2 B_t[h(\lambda_t)]^{-1} \qquad \text{for } t = x, y, z \quad (31)$$

The ratio of birefringence due to constraints to the birefringence of the phantom network is given by combining eqs 16 and 26

$$\Delta n_{xy,c}/\Delta n_{xy,\mathrm{ph}} = \{(B_x - B_y) + b(\lambda_x^2 B_x[h(\lambda_x)]^{-1} - \lambda_y^2 B_y[h(\lambda_y)]^{-1})\}\{1/[1 - (2/\phi)]\}[1/(\lambda_x^2 - \lambda_y^2)] \quad (32)$$

The total birefringence of a real network due to deformation under constraints can then be expressed as

$$\Delta n_{xy} = \Delta n_{xy,\mathrm{ph}}[1 + (\Delta n_{xy,c}/\Delta n_{xy,\mathrm{ph}})] \quad (33)$$

A reduced birefringence analogous to reduced stress can be defined as[7]

$$[\Delta n] = [\Delta n_{\mathrm{ph}}](1 + \Delta n_c/\Delta n_{\mathrm{ph}}) \quad (34)$$

where the reduced phantom birefringence is the product of the reduced phantom modulus and the stress-optical coefficient

$$[\Delta n_{\mathrm{ph}}] = (\xi kT/V_0)C \quad (35)$$

Results and Discussion

Application to Experiment. Consider the application of the theory presented here to a typical strain birefringence experiment. For a network under uniaxial extension, eq 32 can be used in the following modified form

$$\Delta n_c/\Delta n_{\mathrm{ph}} = \{(B_\parallel - B_\perp) + b(\lambda_\parallel^2 B_\parallel[h(\lambda_\parallel)]^{-1} - \lambda_\perp^2 B_\perp[h(\lambda_\perp)]^{-1})\}\{1/[1 - (2/\phi)]\}[1/(\lambda_\parallel^2 - \lambda_\perp^2)] \quad (36)$$

where the subscript "$\parallel$" means parallel to the axis of applied strain and the subscript "$\perp$" means perpendicular to the axis of applied strain. The results of calculations performed using eq 36 are represented in Figure 1. The calculations for a tetrafunctional unswollen network prepared in the bulk have been carried out for four different values of the primary adjustable constraint parameter K_G: 0.1, 1, 5, 50. The two extremes in the value of K_G are not applicable to realistic elastomeric networks but are included to show the predictions of the theory approaching phantom-like and affine-like behavior. The ratio of the birefringence due to constraints to the birefringence of the phantom network is plotted as a function of inverse elongation. The contribution to birefringence of the constraints is at a maximum ($b = 1.0$ in eq 36). The theory predicts sigmoidally shaped curves. The birefringence due to constraints relative to that in the phantom network decreases with elongation as the constraints diminish in the direction of the deformation. The slopes of the curves increase with elongation until reaching a maximum and then begin to decrease as the infinite elongation limit approaches.

Effect of Constraints. The effect of various values of the primary adjustable constraint parameter K_G can be seen in Figure 1, which was previously described. The effect of the secondary constraint scaling parameter, b, can be seen in Figure 2.[16] Figure 2 shows the ratio of the birefringence due to constraints to the birefringence of the phantom network plotted as a function of inverse elongation for three values of the secondary constraint scaling parameter b: 0, 0.5, 1.0. The calculation of the ratio in question from eq 32 was done for a dry, tetrafunctional network prepared in the bulk. The primary adjustable constraint parameter is $K_G = 5.0$, which is a typical value for an elastomeric network.[17] As can be seen in Figure 2, the effect of various values of the secondary constraint scaling parameter, b, is of minor importance compared to the effect of various values of K_G shown in Figure 1. It can also be seen that the effect of parameter b diminishes with elongation, vanishing in the infinite extension limit.

Effect of Swelling. The effect of various degrees of swelling on the predictions of the theory can be seen in Figure 3.[18] The effect of swelling is incorporated into the theory by varying the polymer volume fraction present during experimental measurements, V_2, in eqs 4 and 5. Figure 3 shows the ratio of birefringence due to constraints to the birefringence of the phantom network, calculated from eq 32, as a function of inverse elongation for three values of the polymer volume fraction V_2. The results are representative of a tetrafunctional network prepared in the bulk with $K_G = 5.0$ and $b = 1.0$. The predictions of the theory agree qualitatively with Flory's claim that increased swelling will decrease the constraint contribution to birefringence as a consequence of the decrease of entanglements present within the network.[2,19] There remains a need for more work such as that done recently

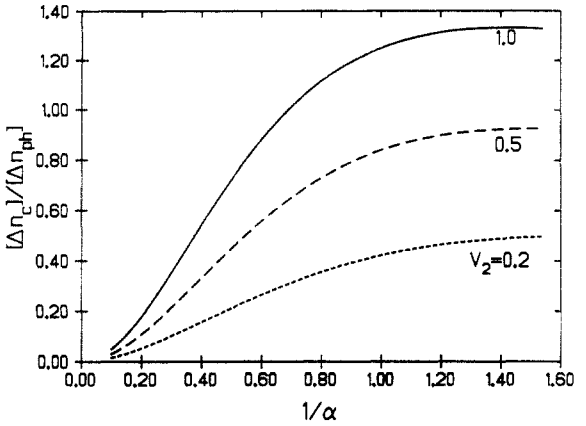

Figure 3. Effect of swelling on representative results. See text for calculation details.

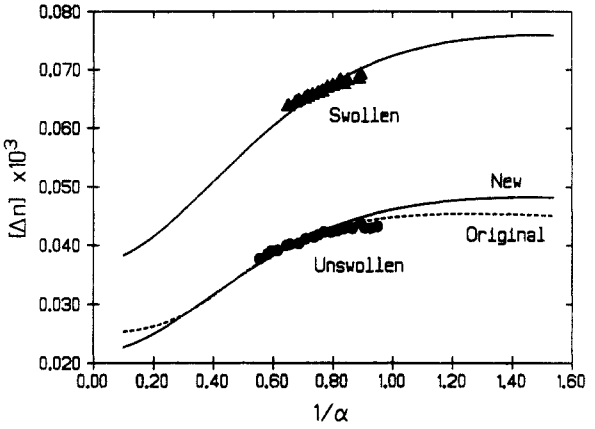

Figure 4. Agreement of theory with data. See text for explanatory details.

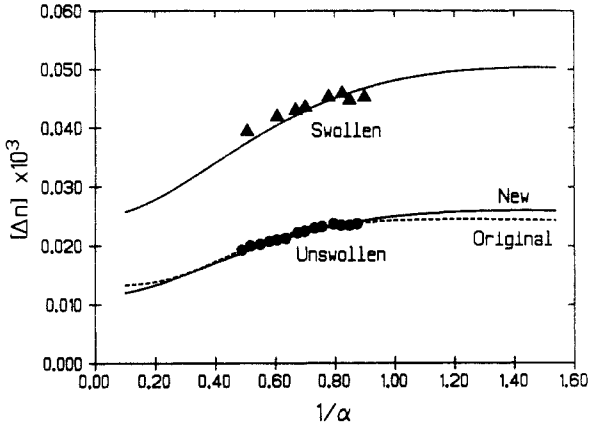

Figure 5. Agreement of theory with data. See text for explanatory details.

by Eman[20] to account for contributions to birefringence from local intermolecular interactions, since such contributions are not included in the predictions of this theory.

Comparison to Experimental Data. Comparisons between the original calculations,[5] previously published experimental data,[21] and the new corrected calculations are shown in Figures 4 and 5. The figures show reduced birefringence as a function of inverse elongation. Equation 32 was substituted into eq 34, and the result was used to generate the lines representing the theoretical predictions. The dashed lines represent the original calculations, and the solid lines represent the new corrected calculations. In Figure 4, the solid circles represent unswollen data previously published by Erman and Flory[21] for poly(dimethylsiloxane) (PDMS), with number-average molecular weight 2×10^6, cross-linked in the bulk with 0.2 wt % dicumyl peroxide. The dashed line representing the original calculation was fit to the unswollen data by selecting a reduced phantom birefringence value of $[\Delta n_{ph}] = 2.51 \times 10^{-5}$, a secondary constraint scaling parameter $b = 0.5$, and $K_G = 5.6$. In comparison, the constrained junction theory was fit to the unswollen data by selecting a reduced phantom birefringence value of $[\Delta n_{ph}] = 2.51 \times 10^{-5}$, $b = 0.5$, $\zeta = 0.05$, and $K = 4.5$. The solid line representing the new calculation was fit to the unswollen data by selecting a reduced phantom birefringence value of $[\Delta n_{ph}] = 2.18 \times 10^{-5}$, a secondary constraint scaling parameter $b = 1.0$, and $K_G = 4.5$. The predicted swelling behavior for a polymer volume fraction $V_2 = 0.78$ was fit to the swollen data[21] (represented by solid triangles) by selecting a reduced phantom birefringence value of $[\Delta n_{ph}] = 3.70 \times 10^{-5}$. In Figure 5, the solid circles represent unswollen data previously published by Erman and Flory[21] for dry PDMS, with number-average molecular weight 2×10^6, cross-linked in the bulk with 0.1 wt % dicumyl peroxide. The dashed line representing the original calculation was fit to the data by selecting a reduced phantom birefringence value of $[\Delta n_{ph}] = 1.32 \times 10^{-5}$, a secondary constraint scaling parameter $b = 0.5$, and $K_G = 8.0$. In comparison, the constrained junction theory was fit to the unswollen data by selecting a reduced phantom birefringence value of $[\Delta n_{ph}] = 1.32 \times 10^{-5}$, $b = 0.5$, $\zeta = 0.05$, and $K = 7.0$. The solid line representing the new calculation was fit to the data by selecting a reduced phantom birefringence value of $[\Delta n_{ph}] = 1.5 \times 10^{-5}$, a secondary constraint scaling parameter $b = 1.0$, and $K_G = 5.5$. The predicted swelling behavior for a polymer volume fraction $V_2 = 0.68$ was fit to the swollen data[21] (represented by solid triangles) by selecting a reduced phantom birefringence value of $[\Delta n_{ph}] = 2.49 \times 10^{-5}$. The corrected terms in the theory were used to calculate the reduced force, and parameters were adjusted by trial and error to produce the best fit to the previously published reduced force data.[21] The K_G values used in Figures 4 and 5 are the same values used for the best fit to the reduced force data. The $[\Delta n_{ph}]$ values used in Figures 4 and 5 were selected to be in the same ratio as the reduced phantom modulus values, $[f^*_{ph}]$, which gave the best fit to the reduced force data. It is necessary to first achieve a best fit to the reduced force data due to the relationship[21]

$$[\Delta n_{ph}] = [f^*_{ph}]C \tag{37}$$

where C is the stress-optical coefficient, which must be a constant for the given networks. Therefore, the $[\Delta n_{ph}]$ values for the unswollen data must be chosen to be in the same ratio as the $[f^*_{ph}]$ values. The swollen data are not subject to this requirement since the value of the stress-optical coefficient, C, will depend on the solvent used. Figures 4 and 5 show that the effect of the corrections made to the original calculations is minimal. Excellent agreement with the data and with previous prediction has been obtained with only minor changes in the adjustable parameters of the theory. The values of the parameters $[\Delta n_{ph}]$ and K_G have been reduced from those used in the original calculations. The values are also smaller than the corresponding values used in the constrained junction model calculations.[21] The new modified calculations from the theory of strain birefringence based on the constrained chain model represent the same strength of network topological constraints with a value of the primary constraint parameter K_G that is lower in magnitude than both the original calculation and the corresponding constrained junction parameter K. Therefore, the primary

constraint parameter K_G in the new calculation is now more sensitive to the strength of network constraints than it was to the original calculation.

Conclusion

The presented strain birefringence theory is molecular in nature and incorporates the effects of topological constraints in a realistic manner based upon the modified constrained chain theory of rubberlike elasticity. The recent corrections made to the modified constrained chain theory of rubberlike elasticity have had little effect on the predictions of the theory of strain birefringence. The new predictions of the theory show excellent agreement with experimental data, as well as with the original predictions, with only minor changes in adjustable parameters. The theory predicts both the swollen and unswollen birefringence behavior equally well. The curves are sigmoidal in shape, with the contribution to birefringence of the constraints relative to that of the phantom network diminishing with elongation. The effect of adjustable parameters on the new corrected predictions of the theory follows the same trend as the original predictions of the theory. A more constrained network (higher constraint parameter K_G) will exhibit a higher contribution to birefringence due to constraints relative to that of the phantom network. Upon increasing the secondary constraint scaling parameter, b, the contribution to birefringence due to constraints relative to that of the phantom network will slightly increase. However, the effect of this parameter is minor in comparison to the effect of primary adjustable constraint parameter K_G, and the effect vanishes at infinite extension.

Although there is debate[3,22] on the contributions made by entanglement constraints to the stress within a network, the entanglements will contribute to the orientation of the network chains upon deformation. It is believed that the secondary constraint scaling parameter, b, is somehow related to this entanglement contribution to orientation, but more work is needed to clearly establish this relationship. It has been suggested[23] that the magnitude of this entanglement contribution to network chain orientation is proportional to M_c/M_e, the ratio of the molecular weight between cross-links to the molecular weight between entanglements. Work has begun to examine this proposed relationship.

Increased swelling significantly diminishes the contribution to birefringence due to constraints relative to that of the phantom network. This supports the premise that swelling decreases the amount of entanglements which would have contributed to the birefringence due to constraints.

The predictions of the presented theory of strain birefringence based on the constrained chain model of rubberlike elasticity[4] will be compared to new data from current strain birefringence experiments on appropriate networks in a future paper. However, the excellent agreement between theory and experimental data previously shown in Figures 4 and 5 supports the validity of the constrained chain theory as a realistic model of rubberlike elasticity.

Acknowledgment. Thanks are due to Prof. B. E. Erman for providing early notification of the corrections made to the constrained chain theory and for suggesting a relationship between M_c/M_e and the entanglement contribution to orientation. Thanks are also due to Dr. A. Kloczkowski for pointing out the error in eq 17. The authors acknowledge the donors of the Petroleum Research Fund, administered by the American Chemical Society, for partial support of this research.

References and Notes

(1) Mark, J. E.; Erman, B. *Rubberlike Elasticity; A Molecular Primer*; Wiley-Interscience: New York, 1988.
(2) Flory, P. J. *J. Chem. Phys.* **1977**, *66*, 5720.
(3) Erman, B.; Flory, P. J. *Macromolecules* **1982**, *15*, 806.
(4) Erman, B.; Monnerie, L. *Macromolecules* **1989**, *22*, 3342.
(5) Galiatsatos, V. *Macromolecules* **1990**, *23*, 3817.
(6) Erman, B.; Mark, J. E. *Macromolecules* **1992**, *25*, 6380.
(7) Erman, B.; Flory, P. J. *Macromolecules* **1983**, *16*, 1601.
(8) Kloczkowski, A.; Mark, J. E.; Sharaf, M. A.; Erman, B. Unpublished.
(9) Pearson, D. S. *Macromolecules* **1977**, *10*, 696.
(10) Ullman, R. *J. Chem. Phys.* **1979**, *71*, 436.
(11) Ullman, R. *Macromolecules* **1982**, *15*, 1393.
(12) Erman, B.; Kloczkowski, A.; Mark, J. E. *Macromolecules* **1989**, *22*, 1432.
(13) Kloczkowski, a.; Mark, J. E.; Erman, B. *Macromolecules* **1989**, *22*, 1423.
(14) Volkenstein, M. W. *Configurational Statistics of Polymeric Chains*; Timasheff, S. N., Timasheff, M. J., Eds.; Interscience: New York, 1963; Chapter 7.
(15) Flory, P. J. *Statistical Mechanics of Chain Molecules*; Interscience: New York, 1969.
(16) Galiatsatos, V. *Polym. Prepr. (Am. Chem. Soc., Div. Polym. Chem.)* **1990**, *31* (2), 683.
(17) Fontaine, F.; Morland, C.; Noel, C.; Monnerie, L.; Erman, B. *Macromolecules* **1989**, *22*, 3348.
(18) Galiatsatos, V. *Polym. Prepr. (Am. Chem. Soc., Div. Polym. Chem.)* **1991**, *32* (2), 679.
(19) Galiatsatos, V. *Trends Polym. Sci.* **1993**, *1*, 20.
(20) Erman, B. Unpublished.
(21) Erman, B.; Flory, P. J. *Macromolecules* **1983**, *16*, 1607.
(22) Ball, R. C.; Doi, M.; Edwards, S. F.; Warner, M. *Polymer* **1981**, *22*, 1010.
(23) Erman, B. Personal communication.